Sea Surface Current Mapping by Radar Doppler Current Profiler

Marius Cysewski
Department of Radar Hydrography
GKSS Research Center
Geesthacht, Germany
marius.cysewski@gkss.de

Dr. Friedwart Ziemer
Department of Radar Hydrography
GKSS Research Center
Geesthacht, Germany
friedwart.ziemer@gkss.de

Dr. Joerg Seemann
Department of Radar Hydrography
GKSS Research Center
Geesthacht, Germany
joerg.seemann@gkss.de

Abstract— **A Radar based method has been developed to measure surface currents directly. Applied techniques, results, capabilities and applications of this method will be discussed.**

Keywords- surface curren mapping; hydrographic radar; radar Doppler spectra; grazing incidence

I. Introduction

Information about the current field is essential for prediction of morphodynamic changes in regions of strong variability in the bathymetry and therefore for the security of ship traffic. An efficient application is also the real-time monitoring of currents in harbours to pilot large vessels. The presented method uses two ship mounted dopplerized X-band radars which scan the speed of scatterers on the water surface during profiling. These radial speeds are corrected by the ship movement and merged by the post-processing software to get a high resolution geo-coded vector map. This method is called, in analogy to the standard current measurement system Acoustic Doppler Current Profiler, ***R**adar **D**oppler **C**urrent **P**rofiler* **RDCP**. The ADCP uses hydro acoustic waves to determine Doppler shift in the vertical water column, RDCP bases on electro magnetic Doppler shift detected on the water surface. The detection of the local variability in the current field like small eddies, convergences and divergences can be mapped [3]. First results of the validation show the accuracy of the latest state of development and allow estimating the tasks in which this method can be usefully applied.

II. Hardware

Commercial nautical X-band radars have been adopted for hydrographic tasks [2]. The dopplerization, A/D converting, the software for radar control and data storage are developed in cooperation with the Technical University of St.Petersburg. Each of the radar transmits 1000 radar pulses per second and the received signals are divided in 254 equidistant range cells with a length of 7.5 m. To avoid interferences, the alternating operation is controlled by the master radar 01 that interlaces every pulse to the slave radar 02. Three different operating modes for the antenna control are possible: rotating antenna (different rotating speeds are possible), stepping antenna (changing of view directions by a table) and to permanently observe a chosen direction. The last option is used for scanning with RDCP where the first radar antenna directed 45° ship ahead and the second 45° aft.

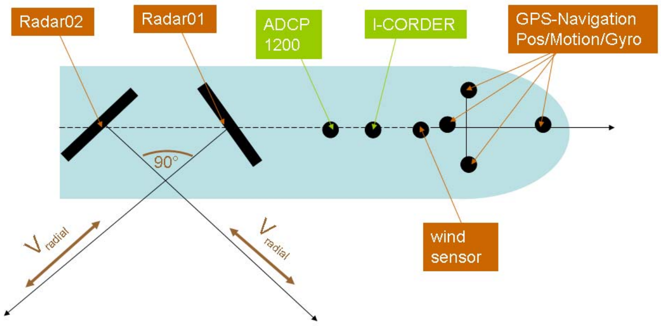

Figure 1. Schema of instrumentation on board a ship for RDCP.

The radar view directions are ship oriented and have to be corrected by heading, ship course and speed over ground for geo-coding as well the impact of ship movement to the scanned radial velocities. A precise two-frequency combining GPS and Glonas navigation system with four antennas is used to measure the following parameters of the ship motion up to 10 Hz: position, heading, roll and pitch.

A weather station mounted approximately ten meters above sea level on the ship mast delivers information regarding the wind speed, direction, air temperature, humidity and global radiation every 6 seconds.

An Acoustic Doppler Current Profiler with frequency of 1200 kHz is used for current measurements below the ship bottom (transducer depth 1.7 m). The ADCP was run with following settings: ensemble time 3 sec, layer depth 0.25 m with a maximum range of 27 m. For the validation campaign an additional 1200 kHz frequency ADCP was mounted on a rubber boat with a transducer depth of 0.5 m.

During the development and research phase a image acquisition system i-corder© took a photo of the water surface every 20 sec which helped to identify indeterminate features in the RDCP maps.

III. Data Processing

Data from each sensor is stored on different computer. Using the radio clock controlled time stamps the pre-processed radar and navigation data is pooled. With FFT a Doppler spectrum is calculated for each of the 254 radial radar cells, see examples Fig. 11,12,13. Integrating over 1 sec with $\Delta f = 1\ Hz$ and λ_{radar}=3cm, the theoretical resolution of determined radial speed results from (1) to ΔV_{radial} = +/- 1.5 cm/s. Spectral moments has been used to find the peak position.

$$\Delta V_{radial} = (\lambda_{radar} / 2) * \Delta f \quad . \qquad (1)$$

The highest measurable frequency is f_{max} = +/-500*Hz*. From (1) follows that the maximum radial speeds are up to ΔV_{radial} = +/- 7.5 m/s.

All the radial speeds from each radial cell are geo-coded for both radars separately. Dead range and orientation offsets for every radar are determined during a reflector calibration using RTK-PDGPS and are applied to each processed data set.

The ship motion is subtracted from the measured radial speeds and geo-coded maps with radial speeds are intermediate result. A first quality check for the dataset and algorithm is the speed control of land parts in the plot, it should be less then 10 cm/s.

By the absolute position of the radial speeds and the absolute view direction of the radar antennas the current vector on 15 m grid is composed.

IV. First Results

For the system development the swell protected area in the tidal channel “Liter Tief” between the north part of the German island “Sylt” and the Danish island Romo is chosen, see Fig. 2. “Sylt” is a hot spot of German activities in the coastal protection. Strong natural morphodynamic changes on shore and in the bathymetry as well as annually beach nourishment has been an additional motivation to test this high resolution surface current mapping system.

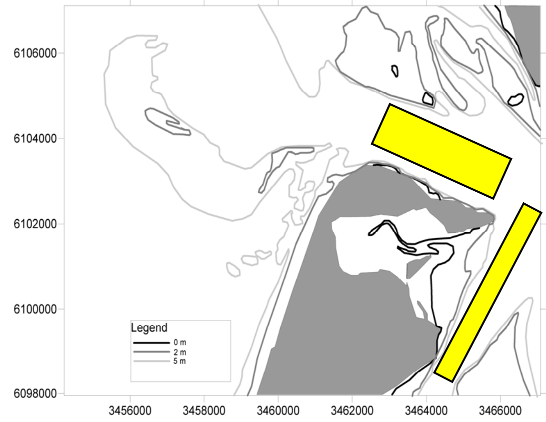

Figure 2. Test area in the tidal channel “Lister Tief” with position of scanned profiles (yellow high lighted). Source of base map “TOP 50 Schleswig-Holstein und Hamburg”.

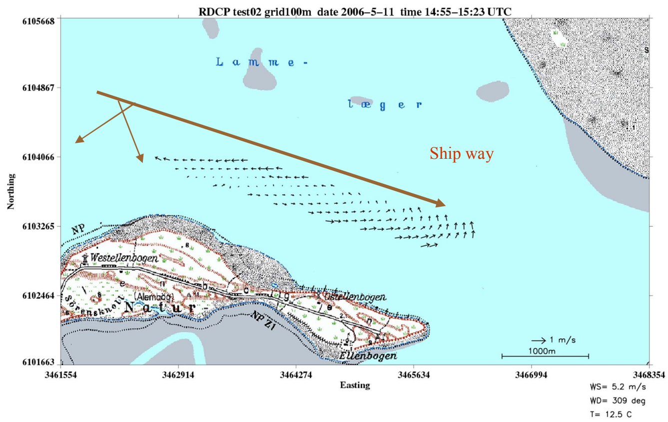

Figure 3. Test area in the tidal channel “Lister Tief”. Black arrows show currents mapped by RDCP during edd tide. Gridresolution 100m. Ship track and the radar antenna view direction are displyed in brown.. Source of base map “TOP 50 Schleswig-Holstein und Hamburg”.

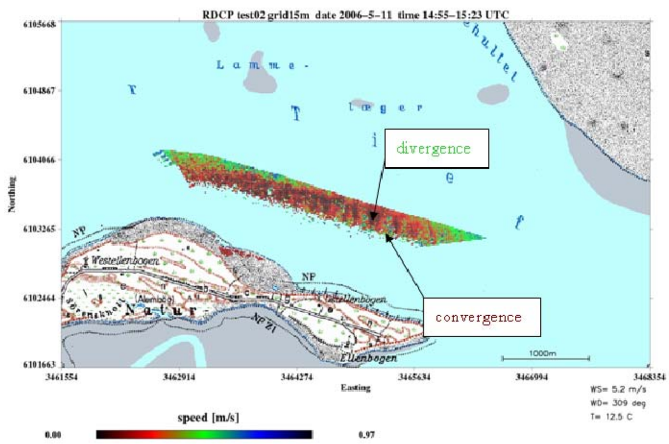

Figure 4. RDCP current map showing the magnitude calculated on 15 m grid. Source of base map “TOP 50 Schleswig-Holstein und Hamburg”.

Fig. 3 shows a current field acquired by RDCP during a campaign in 2006. Because of low wind conditions VV polarization of the radar antennas is used. The flood situation with maximum speed in the center of the channel as well as the out flow direction are visible in the map with a grid resolution of 100 m. The ADCP measurement, acquired during the same track, demonstrates that the calculated RDCP currents have a similar orientation and magnitude.

This current field is overlaid by a current modulation due to the change in the cross section over the submarine sand dunes, which interact with the ebb current. An acceleration above the crest of the dunes and a slowing down where the cross section is widening is observed. Fig. 4 shows these effects on the water surface as plots of magnitude with the actual full spatial resolution of RDCP of about 15m.

Analyzing the RDCP maps an increase of measured magnitudes and rotating directions by rising distance was observed. This lead to the decision to explore the impact of the wind and range impact to the Doppler measurements.

V. WIND-RANGE DEPENDENCY

To determine this wind and range impact, the ship is stopped in areas of homogeneous currents and the radar antennas scan the water surface for 2 sec in 20° steps. The ship motion as well the tidal current are subtracted from the radial measurements, see Fig. 5. The result are radial rays, see Fig, 7, representing the velocity deviation RDCP-ADCP depending on the wind speed, angle between wind and radar antenna view direction as well the distance from the radar.

Each radial ray is fitted and all results are stored after a quality check in an empirically determined look up table sorted by wind speed in steps of 1 m/s. This table contains yet data sets starting by 3 m/s till 15 m/s. Fig. 6 illustrates the schema of the main processing steps.

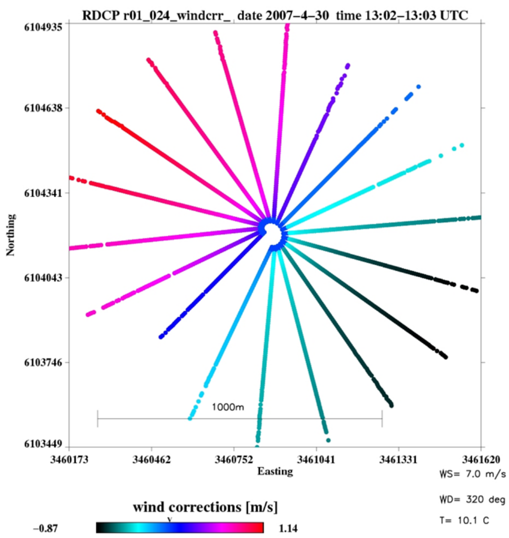

Figure 5. Example of radial RDCP measurments in steps of 20° to determine the wind and range dependency of the velocity corrections for wind speed 7 m/s

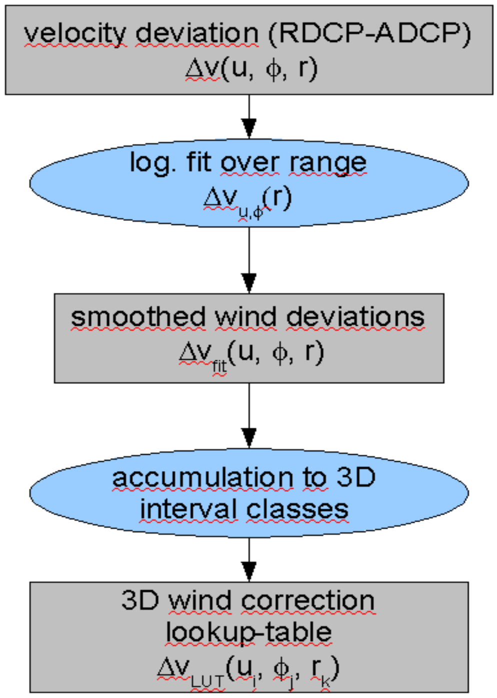

Figure 6. Schema of processing steps for the determination of wind and range dependency

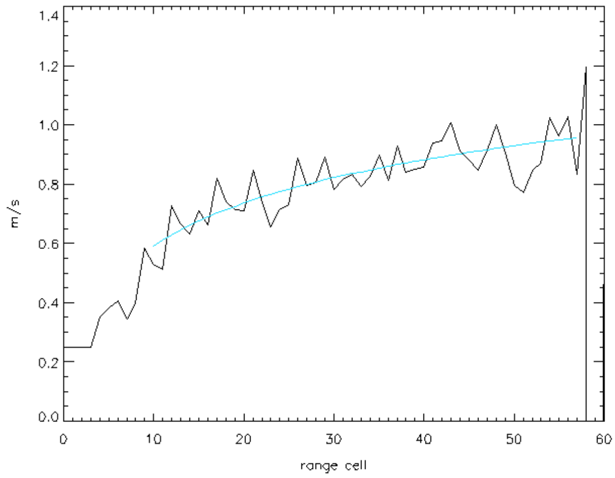

Figure 7. Example of a single radial rdar measurement for radar view direction towarded to the main wind direction. Blue line shows the logarithmic fit over the range

The velocity deviation (RDCP-ADCP) depends on wind speed, wind direction relative to antenna view direction and the distance to the radar. Here the physically relevant parameter is the grazing angle which varies from 6 degrees (near range) to 0.25 degrees (far range). One source for the velocity deviation (RDCP-ADCP) is the wind drift, which was found to be between 0.026 - .055 of U10 (wind speed in 10 m height over water level). From moderate incidence angles to grazing incidence with grazing angles as low as 6 deg it was shown that the velocity deviation between the measured Doppler speed and the current velocity can be accounted to the phase speed of the resonant Bragg waves and the wind drift [4]. In this examination the authors additionally observed a range dependency, which can be accounted to the fact that in far range the sea surface is scanned by the radar beam under very low grazing conditions (as low as 0.25 deg. grazing angle). It was analyzed if there is still a linear relation between the velocity deviation and the wind speed Fig 9 and Fig. 10.

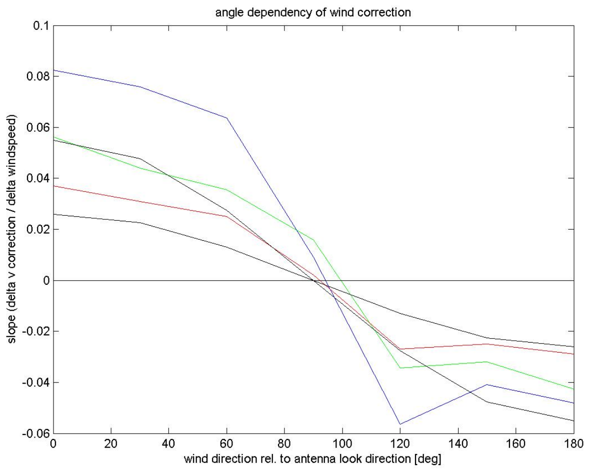

Figure 8. Angle dependency of the wind corrections. Black lines represents the theoretical value 2.6 and 5.5 % of the wind speed. Denpendencies from the look up table: blue for the far range, green for the middle range and red for the near range

In Fig.8 the wind speed directional dependency of the slope of the regression line with should be because of the linear dependency of the wind drift be between 0.026 - 0.055 times cos(rel. wind direction). In the near range the know literature values are verified, but in the far range the slope increases as high as 0.08, i.e. the wind speed sensitivity increases with decreasing grazing angle (see also Fig. 14). In Fig. 11 and Fig. 13 three Doppler spectra with increasingly lower grazing angles are presented. With decreasing grazing angles in addition to an increasing mean Doppler speed the spectrum became broader and splits into 2 components. A similar effect was observed from Lee et al. at low grazing angles with HH polarization. Here it is shown that this effect also appears with VV polarization, but lower grazing angles. The spectral split can be accounted to the occurance of backscattering at microbreakers in addition to the Bragg scattering mechanism. Both the spectral broading and the increased wind speed sensitivity of the Doppler speed deviation are under close examination now to get a closer insight in the backscatter mechanisms at very low grazing angles. Nevertheless the proposed wind speed correction method using the first spectral moment calculated over both Doppler peaks in the far range has to be shown to be very robust and stable.

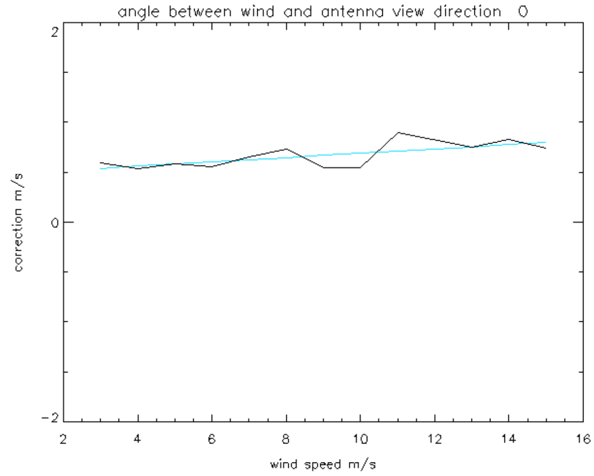

Figure 9. Velocity deviation (RDCP-ADCP) for the distance 75 m. Blue line represents the linear fit over measured wind speeds.

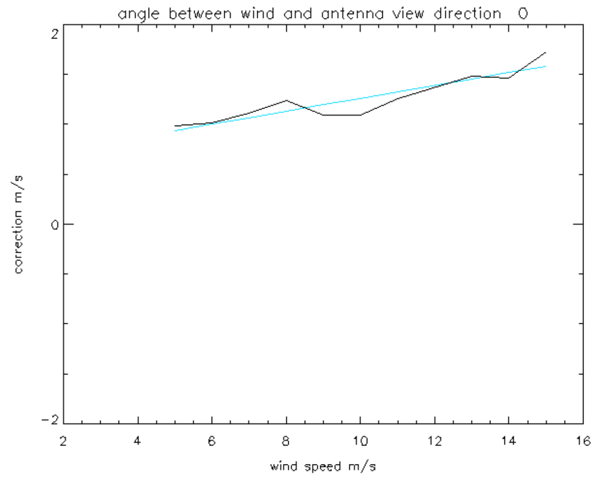

Figure 10. Velocity deviation (RDCP-ADCP) for the distance 660m. Blue line represents the linear fit over measured wind speeds.

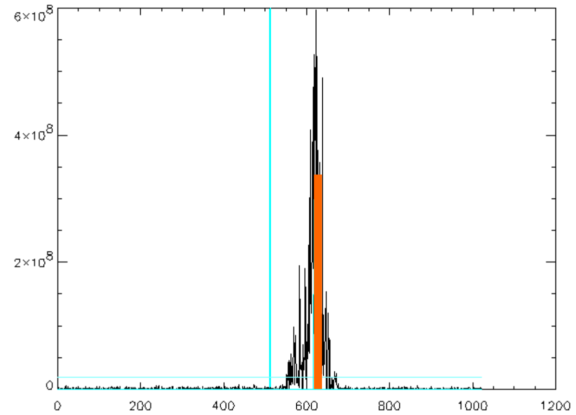

Figure 11. Doppler spectra calulating for 1 sec for a range cell in the distance of 97 m. Blue vertikal line represents 0 Hz. Orange line represents the calculated position of the peak.

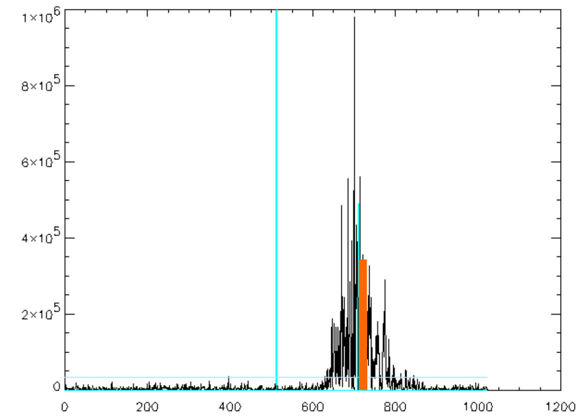

Figure 12. Doppler spectra calulating for 1 sec for a range cell in the distance of 525 m. Blue vertikal line represents 0 Hz. Orange line represents the calculated position of the peak dependency

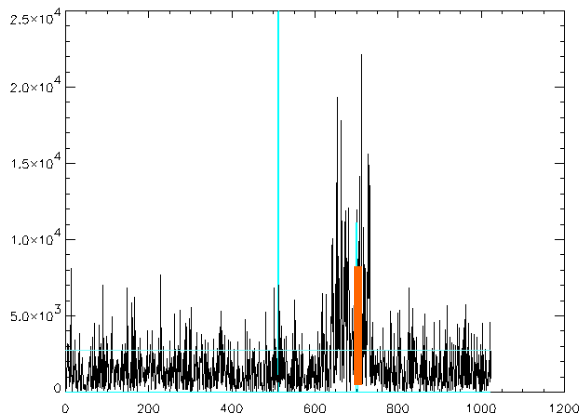

Figure 13. Doppler spectra calulating for 1 sec for a range cell in the distance of 1230 m. Blue vertikal line represents 0 Hz. Orange line represents the calculated position of the peak.

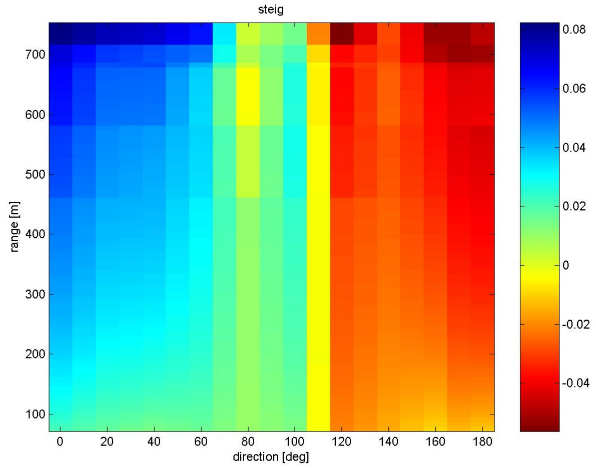

Figure 14. Linaer regression line slope of wind speed dependencies calculated for each radar cell over all measured wind speeds.

VI. APPLIED CORRECTIONS

After applying the corrections from the look up table to each radial ray, the orientation and magnitude of the current vectors change and some new current features appear. Figures 15 and 16 show the same track acquired during the flood tide. The ship track leads from the north east part of “Lister Tief” towards the south part of the harbor List. Fig. 15 demonstrates that the RDCP arrows in the distance of some hundred meters without any corrections are wind and not current orientated. The same track with applied correction reproduces the expected currents and an eddy appears on the water surface, see Fig 16. The existence of this eddy is confirmed by a local sailor.

The comparison of the rubber boat mounted ADCP values (first from depth of 0.5 m) with RDCP measurement, acquired in “Lister Tief” during the same track with a distance between the rubber boat and ship of 450 m, demonstrates that the currents mapped by RDCP have a strong variation, see Fig. 17.

Fig. 18 illustrates the comparison of the RDCP currents with applied wind and range corrections from the empirical look up table and rubber boat mounted ADCP measurement from the same track. The magnitude as well the direction plots show correlations 0.76 for the direction and 0.75 for the magnitude and confirm the need of speed corrections.

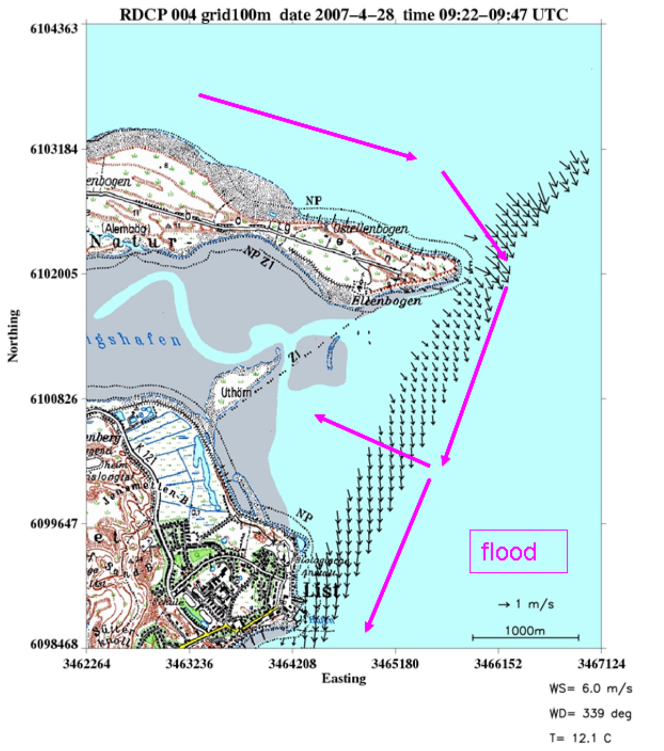

Figure 15. RDCP current map without any correction. Magneta arrows show the typical current situation during the flood tide. Source of base map "TOP 50 Schleswig-Holstein und Hamburg".

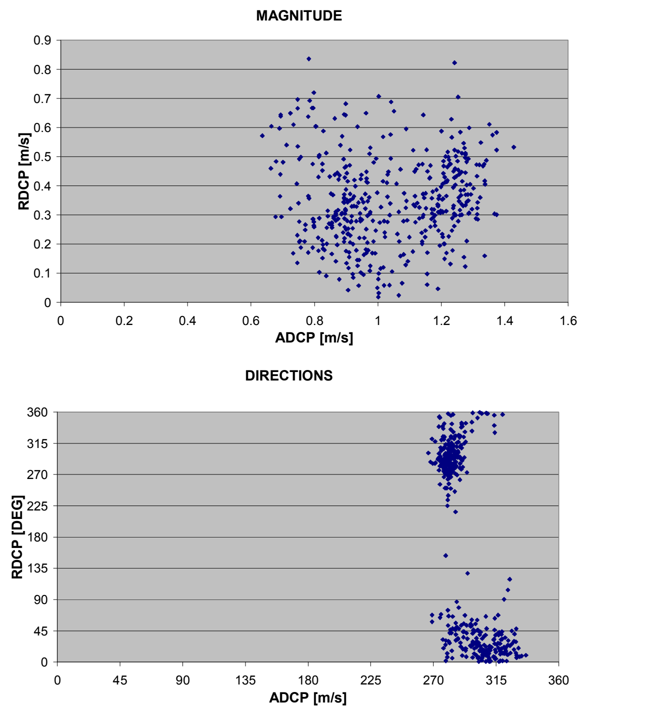

Figure 17. Comparison of the RDCP currents without any corrections and rubber boat mounted ADCP measurement. Both data sets are acquired during the same profile in "Lister Tief". The magnitude as well the direction plots show no correlation.

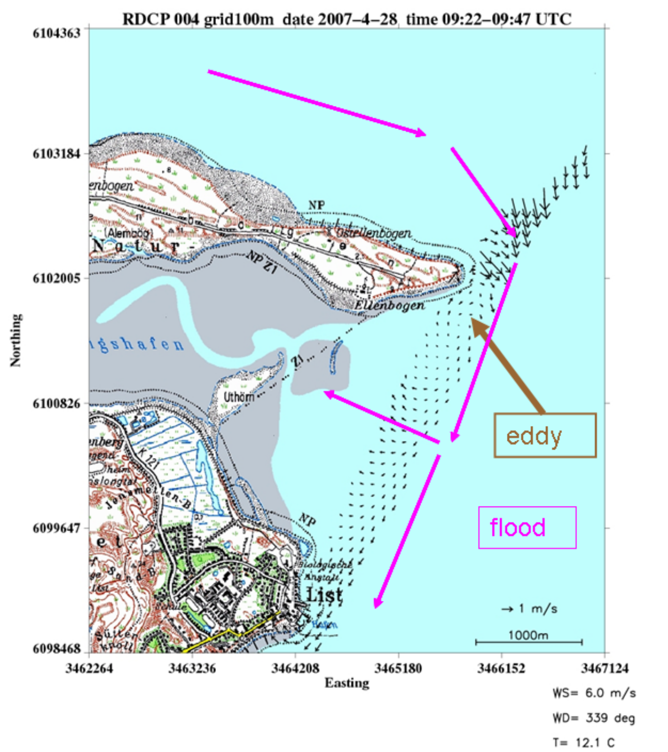

Figure 16. RDCP current map with applied wind and range corrections from the empirical look up table. Magneta arrows show the typical current situation during the flood tide. Source of base map "TOP 50 Schleswig-Holstein und Hamburg".

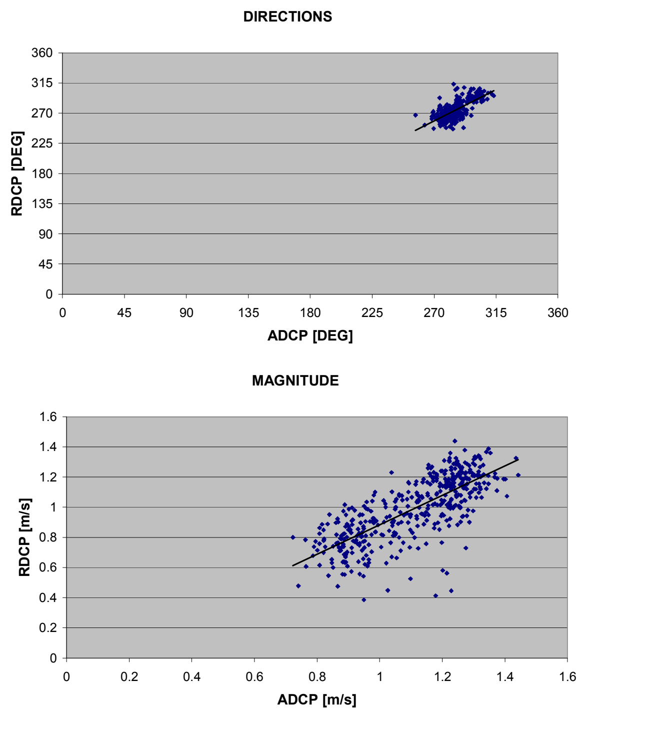

Figure 18. Comparison of the RDCP currents with applied wind and range corrections from the empirical look up table and rubber boat mounted ADCP measurement. Both data sets are acquired during the same profile in "Lister Tief". The magnitude as well the direction plots show correlations 0.76 for the direction and 0.75 for the magnitude.

VII. CONCLUSION AND OUTLOOK

The Radar Doppler Current Profiler is a system designed for geo-coded current mapping measured on the water surface. Small-scale features like eddies, zones of convergences and divergences can be mapped with high resolution in space and time. Closer examination of the empirical wind and range dependencies regarding temperature differences between water and air as well additional parameterization will improve the accuracy of RDCP. Current mapping in port entrances as well between offshore wind mills are possible. For the off shore use the RDCP software has to be complemented by algorithms detecting waves, which impact the radial Doppler measurements.

An additional possible application for RDCP is the use in oil spill fighting. The knowledge about the position of convergences can be used for the optimization of oil skimming. Shifting of tidal gullies can be also mapped as well as the changes of the coast line.

Combining the RDCP current maps with ADCP vertical profiles and bathymetric information areas of potential erosion or deposition can be predicted.

REFERENCES

[1] Allen, N., Trump, C.L.., Trizna, D.B. and D.J. McLaughlin ,"Dual-polarized Doppler radar measurements of oceanic fronts". Geoscience and Remote Sensing, IEEE Transactions on, vol. 37, pp. 395-417, 1999

[2] N.Braun, F. Ziemer, A. Bezuglov and M. Cysewski, "Sea-Surface Current Features Observed by Doppler-Radar", IEEE Transactions on Geoscience and Remote Sensing, Vol 46, No. 4, pp1125 – 1133, 2008

[3] M.Cysewski. and F. Ziemer, "First experiences and applications for Radar Doppler Current Profiler". Hydro 8 International Conference, 4-6 November 2008, Liverpool, UK, 2008

[4] Farquharson, G., Frasier, S.J., Raubenheimer, B. and S. Elgar "Microwave radar cross sections and Doppler velocities measured in the surf zone". J. Geophys. Res., vol. 110, 12/23, 2005

[5] P.H.Y.Lee, et al., "X band microwave backscattering from ocean waves," J. Geophys. Res., vol. 100, NO. C2, pp2591-2611, 1995

[6] P.Lange an H.Huenerfuss, "Drift Response of Monomelucular Slicks to Wave and Wind Action", Journal of Physical Oceanography, Vol. 8, 1977

[7] Plant, W.J., Keller, W.C. & K. Hayes, "Measurement of river surface currents with coherent microwave systems". IEEE Trans. Geosci. Remote Sens., 43, pp. 1242-1257, 2005.

[8] Vogelzang, J., Wensink, G.J., Calkoen, C.J. and M.W.E. Van der Kooij, "Mapping submarine sandwaves with multi-band imaging radar 2. Experimental results and model comparison". Journal of Geophysical Research, 102, pp. 1183-1192.,1997.